FINAL REPORT

NASA-AMES COOPERATIVE AGREEMENT NCC2-5379

MAY 1, 2000 – APRIL 30, 2003

PARABOLIZED NAVIER-STOKES CODE FOR COMPUTING MAGNETO-HYDRODYNAMIC FLOWFIELDS

by

J.C. Tannehill, Principal Investigator
Iowa State University
Ames, IA 50011

Submitted to: National Aeronautics and Space Administration
Ames Research Center
Moffett Field, CA 94035

This final report summarizes the research accomplished under NASA-Ames Cooperative Agreement NCC2-5379 during the period which extended from May 1, 2000 to April 30, 2003. The total funding amounted to $58,000. The Technical Officer for this grant was Dr. Unmeel B. Mehta of NASA Ames Research Center.

The research performed during the grant period is described by the two technical papers (AIAA Papers 2002-0202 and 2003-0326) which are included in this final report.

Computation of Magnetohydrodynamic Flows Using an Iterative PNS Algorithm

Hiromasa Kato*, John C. Tannehill†, Manohari B. Ramesh‡
Iowa State University, Ames, IA 50011
and
Unmeel B. Mehta §
NASA Ames Research Center, Moffett Field, CA 94035

Abstract

A highly efficient numerical algorithm for solving 3-D hypersonic flows with applied electromagnetic fields is being developed. Maxwell's equations of electromagnetodynamics have been added to the PNS equations and the resulting set of equations are solved using a loosely-coupled approach. The fluids and magnetic field equations are decoupled in such a way that the physics of the problem is retained. To account for upstream (elliptic) effects, the flowfields are computed using multiple sweeps with the iterated PNS (IPNS) algorithm. The fluid flow and magnetic field solvers can either be updated independently or coupled iteratively which makes for an efficient approach in dealing with the effects of the magnetic field on the fluid flow. The new algorithm has been used to determine the influence of magnetic fields on two-dimensional hypersonic flows over flat plates and wedges. The present results are in good agreement with previous Navier-Stokes calculations.

Introduction

The recent renewed interest in magnetohydrodynamics (MHD) can be attributed to at least two potential applications. The first is the possibility of reducing supersonic drag and heat transfer by imposing a magnetic field on the ions produced at the bow shock wave [1]. The second is the possibility of increasing the efficiency of hypersonic air-breathing engines by using the energy bypass concept [2]. The MHD energy bypass concept is based on redistributing energy between the various stages of a ramjet/scramjet engine in order to reduce the Mach number at the entrance to the combustion chamber.

Flowfields involving MHD effects have typically been computed [3–8] by solving the complete Navier-Stokes (N-S) equations for fluid flow in conjunction with Maxwell's equations of electromagnetodynamics. When chemical, vibrational and electronic nonequilibrium effects are also included, the computational effort required to solve the resulting coupled system of partial differential equations is extremely formidable. One possible remedy to this problem is to use the parabolized Navier-Stokes (PNS) equations in place of the N-S equations. The PNS equations can be used to predict three-dimensional, hypersonic viscous flowfields in a very efficient manner [9]. This efficiency is achieved because the equations can be solved using a space-marching technique as opposed to the time-marching technique that is normally employed for the complete N-S equations.

One of the most widely-used PNS codes is NASA's upwind PNS (UPS) code which was originally developed by Lawrence et. al [10]. The UPS code solves the PNS equations using a fully conservative, finite-volume approach in a general nonorthogonal coordinate system. The UPS code has been extended to permit the computation of flowfields with strong upstream influences. In regions where strong upstream influences are present, the governing equations are solved using multiple sweeps. As a result of this approach, a complete flowfield can be computed more efficiently (in terms of computer time and storage) than with a standard N-S solver which marches the entire solution in time. Three iterative PNS algorithms (IPNS, TIPNS, and FBIPNS) have been developed. The iterated PNS (IPNS) algorithm [11] can be applied to flows with moderate upstream influences and small streamwise sepa-

*Graduate Research Assistant, Student Member AIAA
†Manager, Computational Fluid Dynamics Center, and Professor, Dept. of AEEM. Fellow AIAA
‡Graduate Research Assistant, Student Member AIAA
§Division Scientist, Associate Fellow, AIAA

rated regions. The time iterated PNS (TIPNS) algorithm [12] can be used to compute flows with strong upstream influences including large streamwise separated regions. The forward-backward sweeping iterative PNS (FBIPNS) algorithm [13] was recently developed to reduce the number of sweeps required for convergence.

In the present study, the UPS code has been extended to permit the computation of two-dimensional/axisymmetric MHD flowfields. Maxwell's equations of electromagnetodynamics have beeen added to the PNS equations and the resulting set of equations are solved using a loosely-coupled approach, similar to that used previously to compute flows in chemical, vibrational, and electronic nonequilibrium [14, 15]. To enhance coupling and also to account for the elliptic character of the MHD equations, the flowfields are computed iteratively using multiple streamwise sweeps with the IPNS algorithm. The resulting code has been tested by computing two cases involving fluid flows with applied electromagnetic fields. These cases include viscous flows over flat plates and inviscid flows over wedges. Comparisons have been made with the previous N-S computations of Hoffmann et al. [7]

Governing Equations

The governing equations for a viscous MHD flow are the Navier-Stokes equations for the flow of the fluid, along with Maxwell's equation of electromagnetodynamics. The equations are given by [7]:

Continuity equation

$$\frac{\partial \rho}{\partial t} + \nabla \cdot (\rho \mathbf{V}) = 0 \tag{1}$$

Momentum equation

$$\frac{\partial (\rho \mathbf{V})}{\partial t} + \nabla \cdot \left[\rho \mathbf{V}\mathbf{V} + \left(p + \frac{B^2}{2\mu_m} \right) \bar{\bar{\mathbf{I}}} - \frac{\mathbf{B}\mathbf{B}}{\mu_m} \right] = \nabla \cdot \bar{\bar{\tau}} \tag{2}$$

Energy equation

$$\frac{\partial (\rho e_t)}{\partial t} + \nabla \cdot \left[\left(\rho e_t + p + \frac{B^2}{2\mu_m} \right) \mathbf{V} - \frac{\mathbf{B}}{\mu_m} (\mathbf{V} \cdot \mathbf{B}) \right] = \nabla \cdot (\mathbf{V} \cdot \bar{\bar{\tau}}) - \nabla \cdot \mathbf{Q} \tag{3}$$

Maxwell's equation

$$\frac{\partial \mathbf{B}}{\partial t} + \nabla \times (\mathbf{V} \times \mathbf{B}) = \nu_m \nabla^2 \mathbf{B} \tag{4}$$

Magnetic field conservation equation

$$\nabla \cdot \mathbf{B} = 0 \tag{5}$$

The flow is assumed to be in chemical equilibrium, and the curve fits of Srinivasan et. al [16, 17] are used for the thermodynamic and transport properties of equilibrium air. Powell's source term [7] is added to the governing equations in order to eliminate the singularity due to the existence of zero eigenvalues of the flow system. The source term, which is proportional to the divergence of the magnetic field is given by

$$\mathbf{H} = \mathbf{H}_M (\nabla \cdot \mathbf{B}) \tag{6}$$

where $\mathbf{H}_M$ is defined later. Since the divergence of the magnetic field is zero, the addition of this source term does not change the governing equations.

The governing equations are nondimensionalized using the following reference variables.

$$x^*, y^* = \frac{x, y}{L}, \quad u^*, v^* = \frac{u, v}{U_\infty}, \quad t^* = \frac{U_\infty t}{L}$$

$$\rho^* = \frac{\rho}{\rho_\infty}, \quad T^* = \frac{T}{T_\infty}, \quad p^* = \frac{p}{\rho U_\infty^2}$$

$$e_t^* = \frac{e_t}{U_\infty^2}, \quad \bar{\bar{\tau}}^* = \frac{\bar{\bar{\tau}} L}{\mu_\infty U_\infty}, \quad \mu^* = \frac{\mu}{\mu_\infty}$$

$$B_x^*, B_y^* = \frac{B_x, B_y}{U_\infty \sqrt{\mu_m \rho_\infty}} \tag{7}$$

$$\mu_m^* = \frac{\mu_m}{\mu_{m_\infty}} = 1, \quad \nu_m^* = \frac{\nu_m}{\nu_{m_\infty}}, \quad \sigma_m^* = \frac{\sigma_m}{\sigma_{m_\infty}}$$

where the superscript $*$ refers to the nondimensional quantities. In subsequent sections, the asterisks are dropped. The magnetic Reynolds number is defined as

$$Re_m = \sigma_{m_\infty} \mu_{m_\infty} U_\infty L$$

The magnetic field equations are then uncoupled from the governing equations of the flow, resulting in one set of equations for the *fluid flow* and another set of governing equations for the *magnetic field*.

Fluid Flow Equations

The vector form of the nondimensionalized governing equations for fluid flow (with magnetic field effects) in a 2-D Cartesian coodinate system are given by

$$\frac{\partial \mathbf{U}}{\partial t} + \frac{\partial \mathbf{E}_i}{\partial x} + \frac{\partial \mathbf{F}_i}{\partial y} + \mathbf{H} = \frac{\partial \mathbf{E}_v}{\partial x} + \frac{\partial \mathbf{F}_v}{\partial y} \tag{8}$$

The vector of the dependent variables is

$$\mathbf{U} = [\rho, \rho u, \rho v, \rho e_t]^T \tag{9}$$

where

$$\rho e_t = \frac{1}{2}\rho V^2 + \frac{p}{\gamma - 1} + \frac{B^2}{2} \tag{10}$$

and the inviscid flux vectors are given by

$$\mathbf{E}_i = \begin{bmatrix} \rho u \\ \rho u^2 + p + \frac{-B_x^2 + B_y^2}{2} \\ \rho uv - B_x B_y \\ \left(\rho e_t + p + \frac{B_x^2 + B_y^2}{2}\right) u \\ -B_x(uB_x + vB_y) \end{bmatrix} \tag{11}$$

$$\mathbf{F}_i = \begin{bmatrix} \rho v \\ \rho vu - B_y B_x \\ \rho v^2 + p + \frac{B_x^2 - B_y^2}{2} \\ \left(\rho e_t + p + \frac{B_x^2 + B_y^2}{2}\right) v \\ -B_y(uB_x + vB_y) \end{bmatrix} \tag{12}$$

Powell's source term for the fluid flow is given by

$$\mathbf{H} = \mathbf{H}_M \left(\frac{\partial B_x}{\partial x} + \frac{\partial B_y}{\partial y}\right) \tag{13}$$

where

$$\mathbf{H}_M = \begin{bmatrix} 0 \\ B_x \\ B_y \\ uB_x + vB_y \end{bmatrix} \tag{14}$$

The viscous flux vectors are given by

$$\mathbf{E}_v = \begin{bmatrix} 0 \\ \tau_{xx} \\ \tau_{xy} \\ u\tau_{xx} + v\tau_{xy} - q_x \end{bmatrix} \tag{15}$$

$$\mathbf{F}_v = \begin{bmatrix} 0 \\ \tau_{yx} \\ \tau_{yy} \\ u\tau_{yx} + v\tau_{yy} - q_y \end{bmatrix} \tag{16}$$

where the nondimensional shear stresses and heat fluxes are defined in the usual manner [7,9].

Magnetic Field Equations

The vector form of the nondimensionalized governing equations for the magnetic field in a 2-D Cartesian coordinate system are given by

$$\frac{\partial \mathbf{B}}{\partial t} + \frac{\partial \mathbf{E}_i^m}{\partial x} + \frac{\partial \mathbf{F}_i^m}{\partial y} + \mathbf{H}^m = \frac{\partial \mathbf{E}_v^m}{\partial x} + \frac{\partial \mathbf{F}_v^m}{\partial y} \tag{17}$$

The solution vector for the magnetic field is

$$\mathbf{B} = \begin{bmatrix} B_x \\ B_y \end{bmatrix} \tag{18}$$

and the inviscid and viscous flux vectors are given by

$$\mathbf{E}_i^m = \begin{bmatrix} 0 \\ uB_y - vB_x \end{bmatrix} \tag{19}$$

$$\mathbf{F}_i^m = \begin{bmatrix} vB_x - uB_y \\ 0 \end{bmatrix} \tag{20}$$

$$\mathbf{E}_v^m = \frac{1}{Re_m \sigma_m} \begin{bmatrix} \frac{\partial B_x}{\partial x} \\ \frac{\partial B_y}{\partial x} \end{bmatrix} \tag{21}$$

$$\mathbf{F}_v^m = \frac{1}{Re_m \sigma_m} \begin{bmatrix} \frac{\partial B_x}{\partial y} \\ \frac{\partial B_y}{\partial y} \end{bmatrix} \tag{22}$$

Powell's source term for the magnetic field is

$$\mathbf{H}^m = \mathbf{H}_M \left(\frac{\partial B_x}{\partial x} + \frac{\partial B_y}{\partial y}\right) \tag{23}$$

where

$$\mathbf{H}_M = \begin{bmatrix} u \\ v \end{bmatrix} \tag{24}$$

Generalized Coordinates

The governing equations for the fluid flow and the magnetic field are transformed into computational space and written in a generalized coordinate system (ξ, η) as

$$\frac{1}{J}\mathbf{U}_t + \mathbf{E}_\xi + \mathbf{F}_\eta + \frac{\mathbf{H}}{J} = 0 \tag{25}$$

$$\frac{1}{J}\mathbf{B}_t + \mathbf{E}_\xi^m + \mathbf{F}_\eta^m + \frac{\mathbf{H}^m}{J} = 0 \tag{26}$$

where

$$\begin{aligned} \mathbf{E} &= \left(\frac{\xi_x}{J}\right)(\mathbf{E}_i - \mathbf{E}_v) + \left(\frac{\xi_y}{J}\right)(\mathbf{F}_i - \mathbf{F}_v) \\ \mathbf{F} &= \left(\frac{\eta_x}{J}\right)(\mathbf{E}_i - \mathbf{E}_v) + \left(\frac{\eta_y}{J}\right)(\mathbf{F}_i - \mathbf{F}_v) \\ \mathbf{E}^m &= \left(\frac{\xi_x}{J}\right)(\mathbf{E}_i^m - \mathbf{E}_v^m) + \left(\frac{\xi_y}{J}\right)(\mathbf{F}_i^m - \mathbf{F}_v^m) \\ \mathbf{F}^m &= \left(\frac{\eta_x}{J}\right)(\mathbf{E}_i^m - \mathbf{E}_v^m) + \left(\frac{\eta_y}{J}\right)(\mathbf{F}_i^m - \mathbf{F}_v^m) \end{aligned} \tag{27}$$

PNS Equations

The fluid flow equations with magnetic field effects [Eq. (25)] are parabolized by dropping the time derivative term and the streamwise (ξ direction viscous flow terms in the flux vectors. Equation (25) can then be rewritten as

$$\mathbf{E}_\xi + \mathbf{F}_\eta + \frac{\mathbf{H}}{J} = 0 \tag{28}$$

where

$$\begin{aligned} \mathbf{E} &= \left(\frac{\xi_x}{J}\right)\mathbf{E}_i + \left(\frac{\xi_y}{J}\right)\mathbf{F}_i \\ \mathbf{F} &= \left(\frac{\eta_x}{J}\right)(\mathbf{E}_i - \mathbf{E}_v') + \left(\frac{\eta_y}{J}\right)(\mathbf{F}_i - \mathbf{F}_v') \end{aligned} \tag{29}$$

The prime in the preceding equation indicates that the streamwise viscous flow terms have been dropped.

Numerical Solution

The MHD flow is solved using a loosely-coupled approach, wherein the fluid flow and magnetic field problems are separated from each other. The resulting system of equations are coupled through the momentum and energy equations. The effects of the magnetic field are manifested in the momentum equations through the electromagnetic forces, and in the energy equation. The effects of the velocity field appear in the convective terms of the magnetic field equations.

The IPNS flow solver is first used to obtain a velocity profile at each streamwise station. This solution is then used in the magnetic field equations to determine the magnetic field profile. The above process is repeated at each streamwise station until a complete (initial) sweep of the flowfield is made. Subsequent sweeps of the flowfield utilize downstream information from the previous sweep (at each station) to account for upstream (elliptic) effects. This iterative procedure is continued until a converged solution is obtained.

Fluid Flow Solver

The iterative PNS (IPNS) method [11] has been modified to solve the PNS equations with magnetic field terms included, i.e. Eq. (28). The $\mathbf{E}$ vector is split using a modified Vigneron parameter ω^m. This parameter accounts for the magnetic field effects on the ellipticity of the flow, and is given by

$$\omega^m = \min\left[1, \frac{\gamma M_x^2}{1+(\gamma-1)\left(M_x^2+\frac{B_y^2}{\rho a^2}\right)}\right] \tag{30}$$

where $M_x = u/a$ and a is the nondimensional speed of sound. This parameter is derived assuming $B_x = 0$ and $v << u$. As a result, $\mathbf{E}$ can be written

$$\mathbf{E} = \mathbf{E}^* + \mathbf{E}^p \tag{31}$$

where

$$\mathbf{E}^* = \frac{\xi_x}{J}\begin{bmatrix} \rho u \\ \rho u^2 + \omega^m p + \frac{B_y^2 - B_x^2}{2} \\ \rho uv - B_x B_y \\ \left(\rho e_t + p + \frac{B_y^2 - B_x^2}{2}\right) u - B_x B_y v \end{bmatrix} + \frac{\xi_y}{J}\begin{bmatrix} \rho v \\ \rho uv - B_x B_y \\ \rho v^2 + \omega^m p + \frac{B_x^2 - B_y^2}{2} \\ \left(\rho e_t + p + \frac{B_x^2 - B_y^2}{2}\right) v - B_x B_y u \end{bmatrix}$$

$$\mathbf{E}^p = \frac{\xi_x}{J}\begin{bmatrix} 0 \\ (1-\omega^m)p \\ 0 \\ 0 \end{bmatrix} + \frac{\xi_y}{J}\begin{bmatrix} 0 \\ 0 \\ (1-\omega^m)p \\ 0 \end{bmatrix} \tag{32}$$

The streamwise derivative of $\mathbf{E}$ is then differenced using a forward difference for the "elliptic" portion ($\mathbf{E}^p$):

$$\left(\frac{\partial \mathbf{E}}{\partial \xi}\right)_{i+1} = \frac{1}{\Delta\xi}\left[\left(\mathbf{E}^*_{i+1} - \mathbf{E}^*_i\right) + \left(\mathbf{E}^p_{i+2} - \mathbf{E}^p_{i+1}\right)\right] \tag{33}$$

where the subscript $(i+1)$ denotes the spatial index (in the ξ direction) where the solution is currently being computed. The vectors $\mathbf{E}^*_{i+1}$ and $\mathbf{E}^p_{i+1}$ are then linearized in the following manner:

$$\begin{aligned} \mathbf{E}^*_{i+1} &= \mathbf{E}^*_i + \left(\frac{\partial \mathbf{E}^*}{\partial \mathbf{U}}\right)_i (\mathbf{U}_{i+1} - \mathbf{U}_i) \\ &\quad + \left(\frac{\partial \mathbf{E}^*}{\partial \mathbf{B}}\right)_i (\mathbf{B}_{i+1} - \mathbf{B}_i) \\ \mathbf{E}^p_{i+1} &= \mathbf{E}^p_i + \left(\frac{\partial \mathbf{E}^p}{\partial \mathbf{U}}\right)_i (\mathbf{U}_{i+1} - \mathbf{U}_i) \\ &\quad + \left(\frac{\partial \mathbf{E}^p}{\partial \mathbf{B}}\right)_i (\mathbf{B}_{i+1} - \mathbf{B}_i) \end{aligned} \tag{34}$$

The Jacobians can be represented by

$$\begin{aligned} A^* &= \left.\frac{\partial \mathbf{E}^*}{\partial \mathbf{U}}\right|_{\mathbf{B}} \\ A^{*m} &= \left.\frac{\partial \mathbf{E}^*}{\partial \mathbf{B}}\right|_{\mathbf{U}} \\ A^p &= \left.\frac{\partial \mathbf{E}^p}{\partial \mathbf{U}}\right|_{\mathbf{B}} \\ A^{pm} &= \left.\frac{\partial \mathbf{E}^p}{\partial \mathbf{B}}\right|_{\mathbf{U}} \end{aligned} \tag{35}$$

After substituting the above linearizations into Eq. (33), the expression for the streamwise gradient of $\mathbf{E}$ becomes

$$\begin{aligned} \left(\frac{\partial \mathbf{E}}{\partial \xi}\right)_{i+1} &= \frac{1}{\Delta\xi}\Big[\left(A^*_i - A^p_i\right)(\mathbf{U}_{i+1} - \mathbf{U}_i) \\ &\quad + \left(A^{*m}_i - A^{pm}_i\right)(\mathbf{B}_{i+1} - \mathbf{B}_i) \\ &\quad + \left(\mathbf{E}^p_{i+2} - \mathbf{E}^p_i\right)\Big] \end{aligned} \tag{36}$$

The final discretized form of the fluid flow equations with magnetic field effects is obtained by substituting Eq. (36) into Eq. (28) along with the linearized expression for the flux in the cross flow plane. The final expression becomes:

$$\left[\frac{1}{\Delta\xi}\left(A_i^* - A_i^p\right) + \frac{\partial}{\partial\eta}\left(\frac{\partial \mathbf{F}}{\partial \mathbf{U}}\right)_i\right]^{k+1} (\mathbf{U}_{i+1} - \mathbf{U}_i)^{k+1} = \mathbf{RHS} \tag{37}$$

where

$$\begin{aligned}\mathbf{RHS} = & -\frac{1}{\Delta\xi}\Big[(A_i^{*m} - A_i^{pm})^k(\mathbf{B}_{i+1} - \mathbf{B}_i)^k \\ & + (\mathbf{E}_{i+2}^p)^k - (\mathbf{E}_i^p)^{k+1}\Big] \\ & - \frac{\partial}{\partial\eta}\left[\left(\frac{\partial \mathbf{F}}{\partial \mathbf{B}}\right)_i^k (B_{i+1} - B_i)^k\right] \\ & - \left(\frac{\partial \mathbf{F}}{\partial\eta}\right)_i^{k+1} - \left(\frac{\mathbf{H}}{J}\right)_{i+1}^k\end{aligned}$$

and the superscript k+1 denotes the current iteration (i.e. sweep) level.

Magnetic Field Solver

The magnetic field equations [Eq. (26)] are solved at each streamwise station $(i+1)$ after the fluid flow equations have been solved using the algorithm described in the previous section. Thus, the velocity components, u and v, are known at station $(i+1)$. The unsteady magnetic field equations are then solved using the Euler implicit scheme [9]. Typically, 5-10 time steps are required to converge the solution at each station. This solution yields the B_x and B_y profiles in the crossflow plane at station $(i+1)$. These values of B_x and B_y can then be put back into the fluid flow solver to recompute values of u and v at the current station in a predictor-corrector fashion. These corrected values of u and v can then be used in the magnetic field solver to recompute values of B_x and B_y at the $(i+1)$ station.

Numerical Results

In order to investigate the utility and accuracy of the present approach of solving an MHD flowfield in a loosely-coupled fashion, a few basic test cases were computed. The hypersonic flow in these cases was altered by the presence of the magnetic field which is applied to the flow.

Test Case 1: Hypersonic flow over a flat plate with applied magnetic field

This test case corresponds to the flat plate test case of Hoffmann et al. [7], wherein the air flow is hypersonic, viscous, and in chemical equilibrium. The flat plate is maintained at a constant temperature and a fixed magnetic field is applied at the inflow boundary. Along the flat plate, the magnetic field is determined by specifying that the normal gradients of the magnetic field components are zero. Likewise, zero gradients of the magnetic field components are assumed at the top and outflow boundaries. A schematic of this test case is given in Figure 1. The dimensional flow parameters for this test case are

$$\begin{aligned} M_\infty &= 10.0 \\ p_\infty &= 1013.3 \text{ N/m}^2 \\ T_\infty &= T_{\text{wall}} = 1950 \text{ K} \\ (B_x)_\infty &= 0.0 \\ (B_y)_\infty &= B_0 = 0.25 \times 10^{-3} \text{ T}, \quad 0.50 \times 10^{-3} \text{ T} \\ L &= 1.0 \text{ m} \\ \sigma_m &= (1/9) \times 10^{11} \text{ mho/m} \end{aligned}$$

For this case, an extremely large constant value of electrical conductivity is specified which makes the fluid nearly infinitely conducting. It should be noted that Hoffmann et al. [7] erroneously give a value for the electrical conductivity of 100 mho/m for this test case.

A highly stretched grid consisting of 100 points in the normal direction was used to compute this case. The first point off the wall was located at 5×10^{-5} m. Figure 2 shows a comparison of the x-component velocity profile at x/L = 0.99 for different values of B_0. The present results compare very well with the Navier-Stokes results of Hoffmann et al. As can be seen in the figure, the boundary layer grows as the magnetic field strength is increased. A comparison of the temperature profiles at x/L = 0.99 is shown in Fig. 3. The present results agree closely with those of Hoffmann et al., although slight differences can be detected even for the case of no applied magnetic field. The present results were computed using equilibrium air curve fits [16,17] for *both* the thermodynamic and transport properties and this may explain the small differences. Profiles of the magnetic field components B_x and B_y are compared in Figs. 4 and 5 at x/L = 0.99. The present results are in reasonable agreement with the N-S results of Hoffmann et al.

Test Case 2: Hypersonic flow over a wedge with applied magnetic field

The second test case considered involves the steady hypersonic 2-D flow of an inviscid, infinitely conducting fluid past a non-conducting wedge. This test case corresponds to the one solved previously by Hoffmann et al. [7] A rectilinear, uniform magnetic field which is constant along the surface of the wedge is applied in a direction orthogonal to the freestream. A schematic of this test case is given in Fig. 6. The flow parameters for this test case are

$$\begin{aligned} \theta &= 5^\circ \\ M_\infty &= 10.0 \\ p_\infty &= 299.8\ \mathrm{N/m^2} \\ T_\infty &= 260.91\ \mathrm{K} \\ (B_x)_{\mathrm{wall}} &= 0.0 \\ (B_y)_{\mathrm{wall}} &= B_0 = 0.05\ \mathrm{T} \end{aligned}$$

The pressure and temperature profiles are presented in Figures 7 and 8, for zero angle of attack. Comparisons are made with the numerical solution of Hoffmann et al. [7]. It can be seen that there is good agreement between the current pressure results and the results of Hoffmann et al. Computations involving larger values of B_0 are currently underway.

Concluding Remarks

Although only limited results have been obtained thus far, it can be seen that the present approach of decoupling the magnetic problem from the fluid flow problem, and solving them in an iterative manner is quite promising. Computations of other test cases are currently underway in order to validate the accuracy of the current method in a variety of flow situations including internal flows.

Acknowledgments

This work was supported by NASA Ames Research Center under Grant NCC2-5379 and by Iowa State University. The Technical Monitor for the NASA grant is Dr. Unmeel B. Mehta.

References

[1] Candler, G. V. and Kelly, J. D., "Effect of Internal Energy Excitation on Supersonic Blunt-Body Drag," AIAA Paper 99-0418, Jan. 1999.

[2] Chase, R. L., Mehta, U. B., Bogdanoff, D. W., Park, C., Lawrence, S. L., Aftosmis, M. J., Macheret, S., and Shneider, M., "Comments on an MHD Energy Bypass Engine Powered Spaceliner," AIAA Paper 99-4975, Nov. 1999.

[3] MacCormack, R. W., "An Upwind Conservation Form Method for the Ideal Magneto-Hydrodynamics Equations," AIAA Paper 99-3609, June 1999.

[4] Deb, P. and Agarwal, R., "Numerical Study of Compressible Viscous MHD Equations with a Bi-Temperature Model for Supersonic Blunt Body Flows," AIAA Paper 2000-0449, Jan. 2000.

[5] Munipalli, R., Anderson, D. A., and Kim, H., "Two-Temperature Computations of Ionizing Air with MHD Effects," AIAA Paper 2000-0450, Jan. 2000.

[6] Damevin, H. M., Dietiker, J.-F., and Hoffmann, K. A., "Hypersonic Flow Computations with Magnetic Field," AIAA Paper 2000-0451, Jan. 2000.

[7] Hoffmann, K. A., Damevin, H. M., and Dietiker, J.-F., "Numerical Simulation of Hypersonic Magnetohydrodynamic Flows," AIAA Paper 2000-2259, June 2000.

[8] Deb, P. and Agarwal, R., "Numerical Study of MHD-Bypass Scramjet Inlets with Finite-Rate Chemistry," AIAA Paper 2001-0794, Jan. 2001.

[9] Tannehill, J. C., Anderson, D. A., and Pletcher, R. H., *Computational Fluid Mechanics and Heat Transfer*, Taylor and Francis, Washington, D.C., 1997.

[10] Lawrence, S. L., Tannehill, J. C., and Chaussee, D. S., "Upwind Algorithm for the Parabolized Navier-Stokes Equations," *AIAA Journal*, Vol. 27, No. 9, Sept. 1989, pp. 1975–1983.

[11] Miller, J. H. and Tannehill, J. C., "PNS Algorithm for Solving Supersonic Flows with Upstream Influences," AIAA Paper 98-0226, Jan. 1998.

[12] Tannehill, J. C., Miller, J. H., and Lawrence, S. L., "Development of an Iterative PNS Code for Separated Flows," AIAA Paper 99-3361, June 1999.

[13] Kato, H. and Tannehill, J. C., "Development of a Forward-Backward Sweeping Parabolized Navier-Stokes Algorithm," AIAA Paper 2002-0735, Jan. 2002.

[14] Buelow, P. E., Tannehill, J. C., and Ievalts, J. O., "A Three-Dimensional Upwind Parabolized Navier-Stokes Code for Chemically Reacting Flows," *Journal of Thermophysics and Heat Transfer*, Vol. 5, No. 3, July-Sept. 1991, pp. 274–283.

[15] Miller, J. H., Tannehill, J. C., Lawrence, S. L., and Edwards, T. A., "Parabolized Navier-Stokes Code for Hypersonic Flows in Thermo-Chemical Equilibrium or Nonequilibrium," *Computers and Fluids*, Vol. 27, No. 2, 1998, pp. 199–215.

[16] Srinivasan, S., Tannehill, J. C., and Weilmuenster, K. J., "Simplified Curve Fits for the Thermodynamic Properties of Equilibrium Air," NASA RP 1181, Aug. 1987.

[17] Srinivasan, S., Tannehill, J. C., and Weilmuenster, K. J., "Simplified Curve Fits for the Transport Properties of Equilibrium Air," NASA CR 178411, 1987.

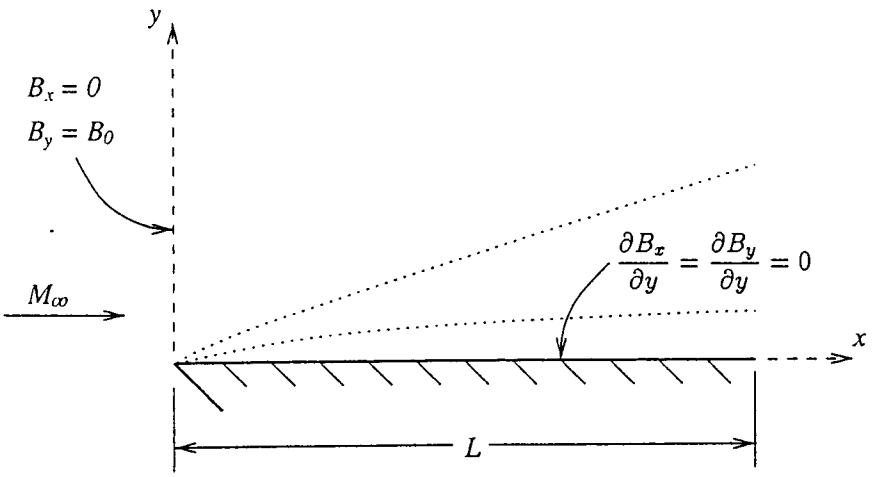

Figure 1: Test Case 1

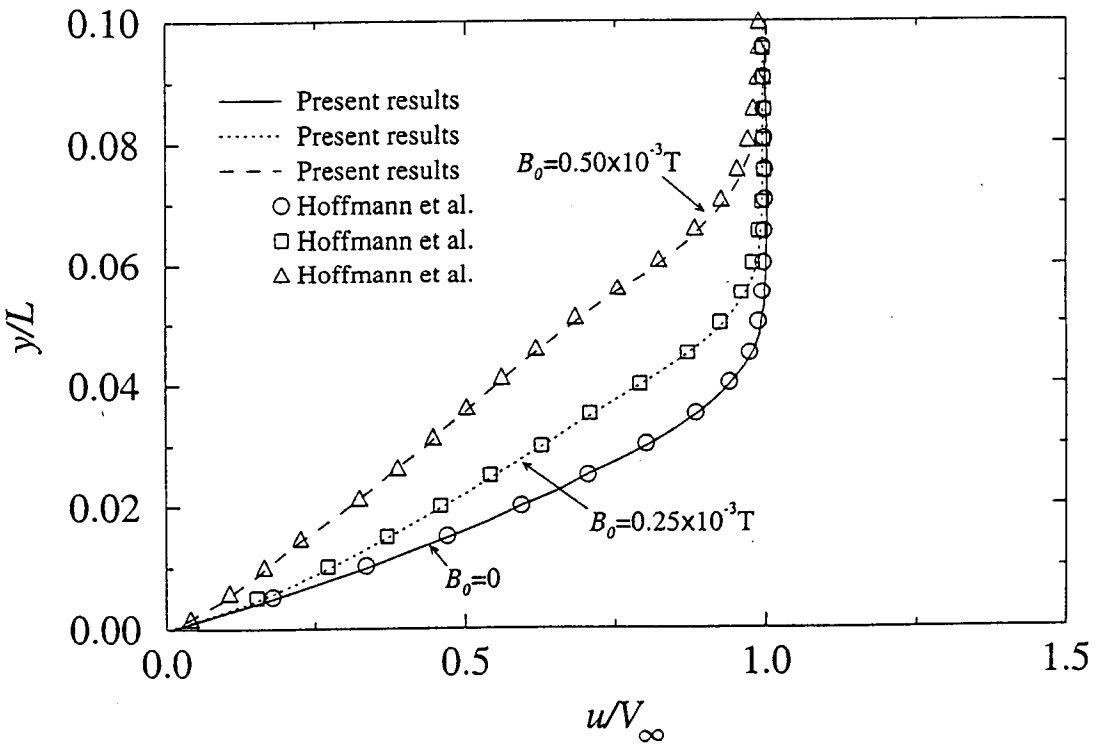

Figure 2: Velocity profiles

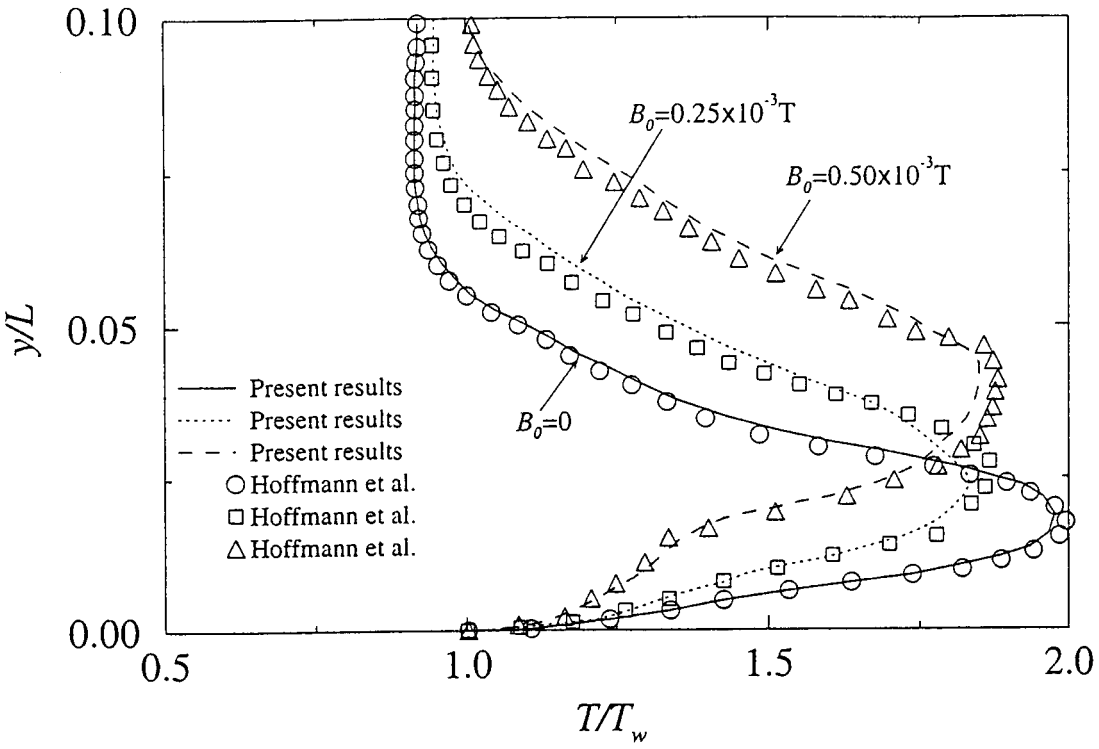

Figure 3: Temperature profiles

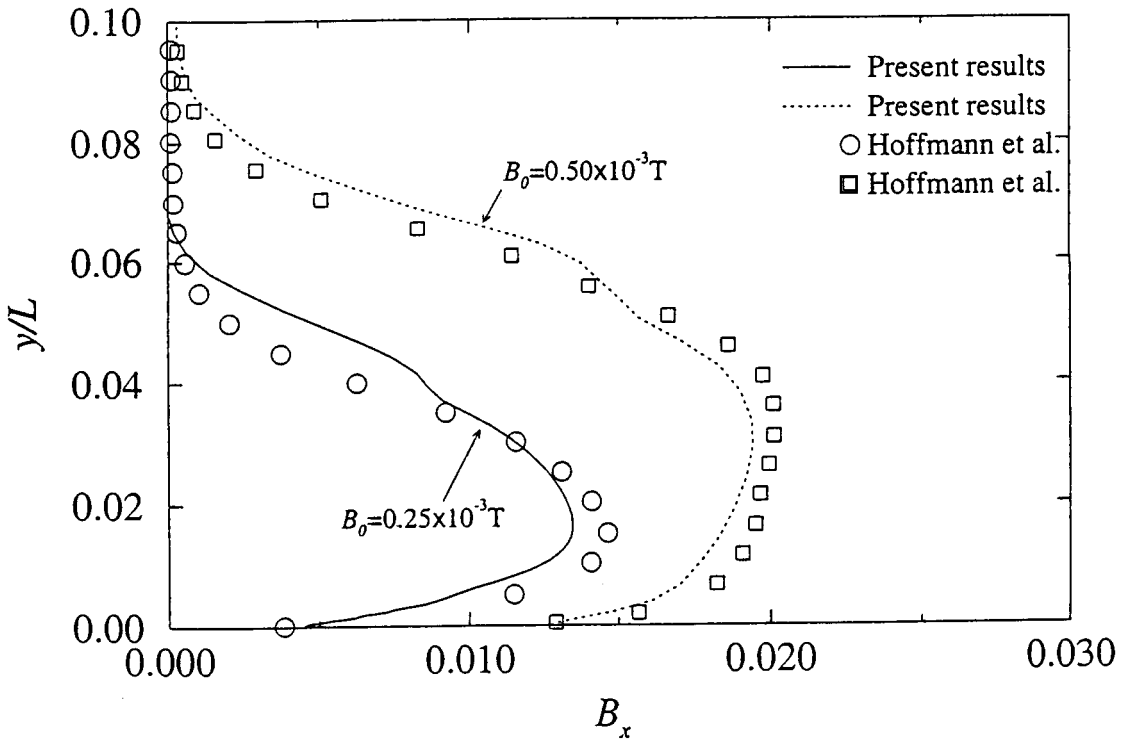

Figure 4: Magnetic field (x-component) profiles

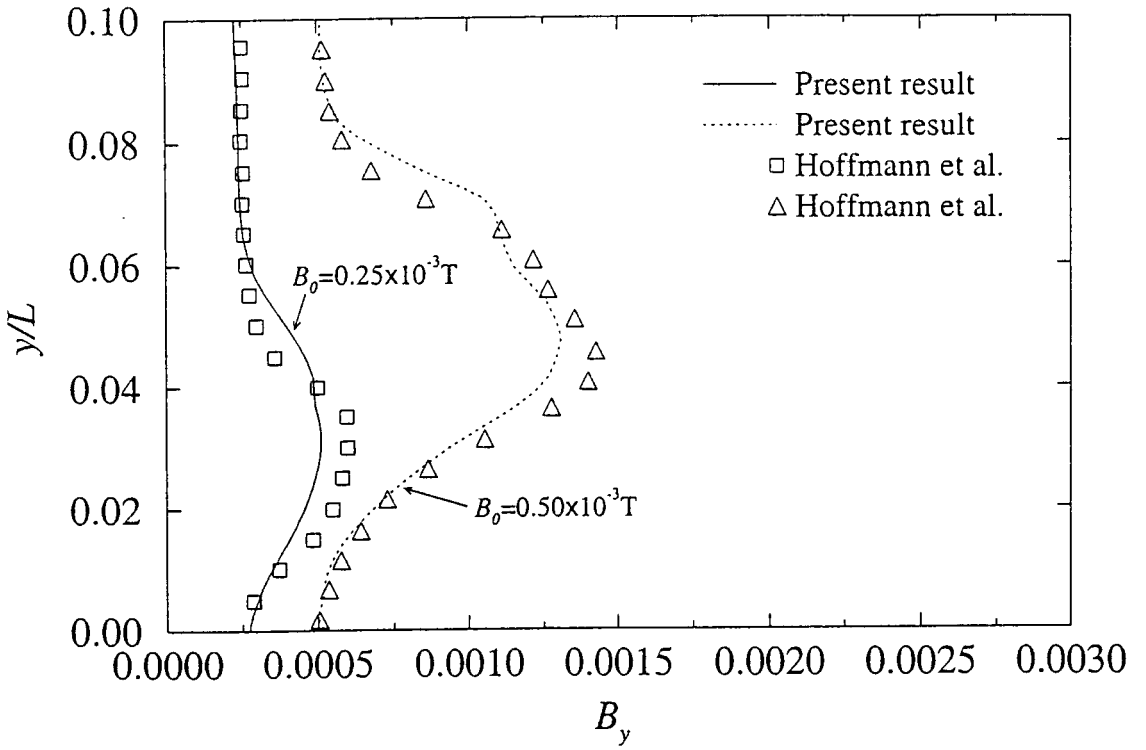

Figure 5: Magnetic field (y-component) profiles

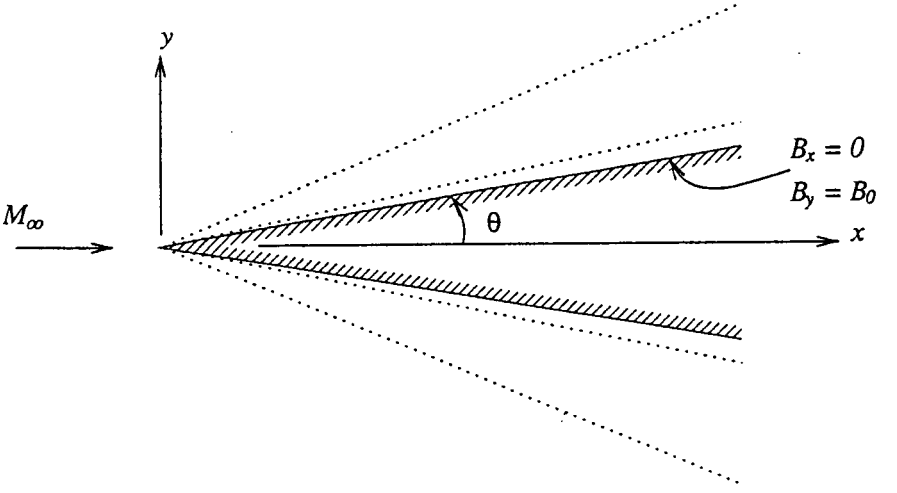

Figure 6: Test Case 2

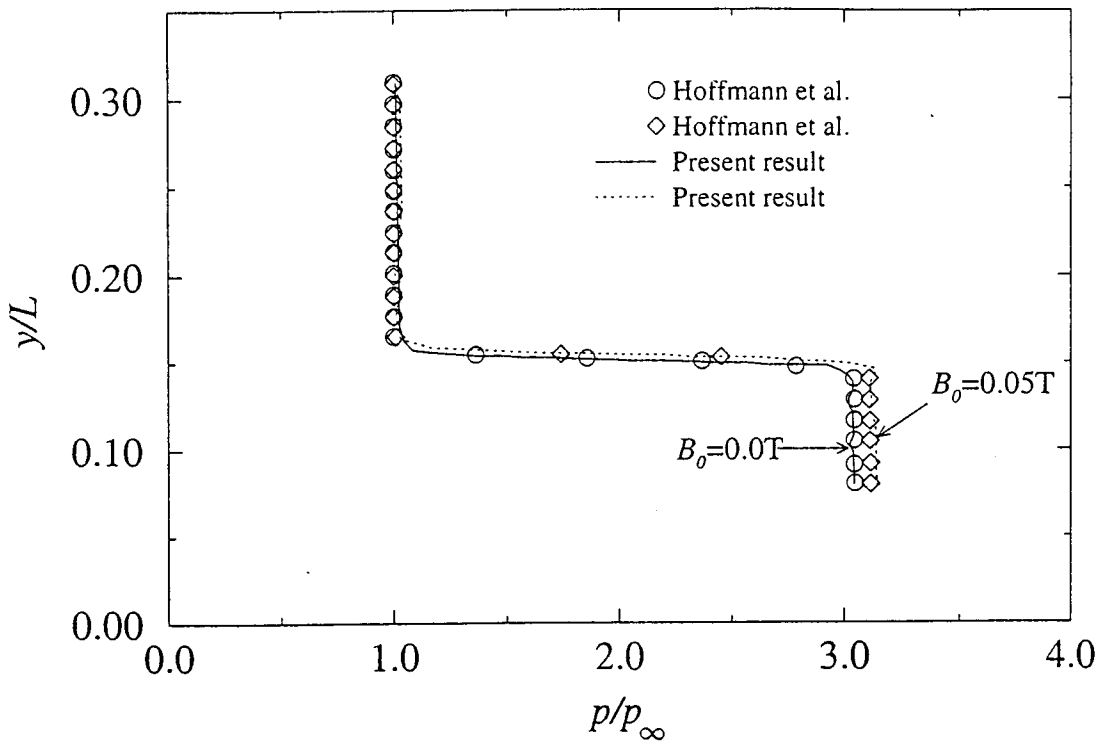

Figure 7: Pressure profile

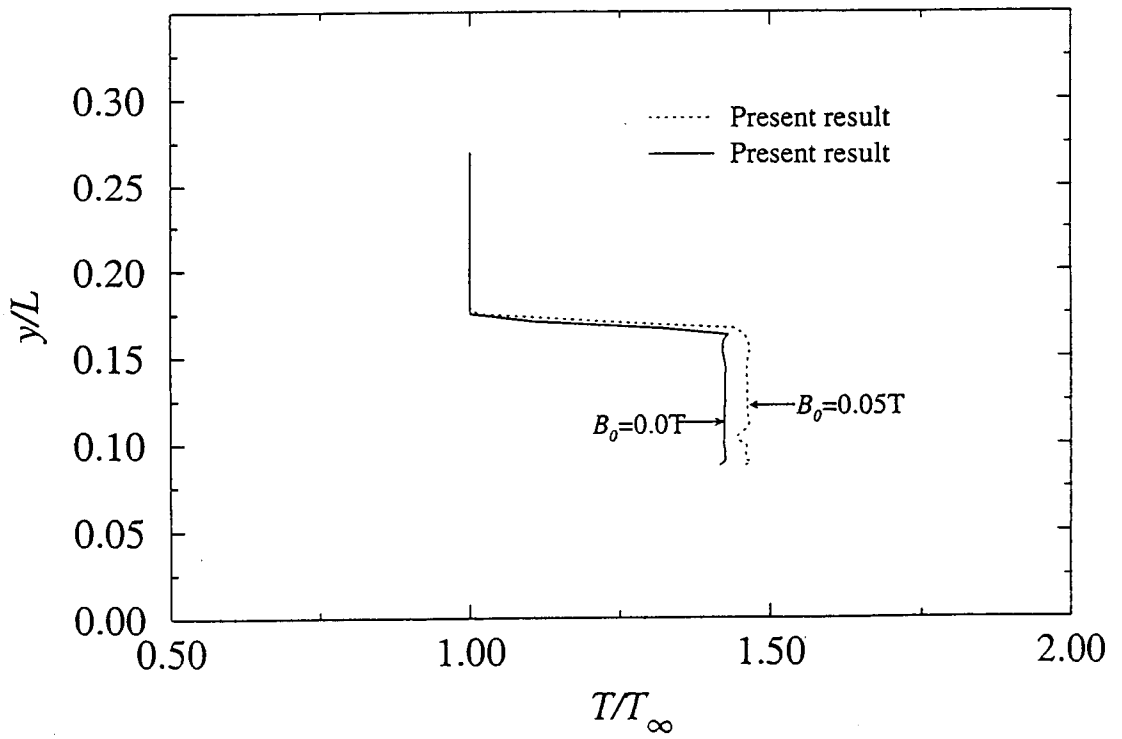

Figure 8: Temperature profile

Numerical Simulation of Turbulent MHD Flows Using an Iterative PNS Algorithm

Hiromasa Kato* and John C. Tannehill†
Iowa State University, Ames, IA 50011
and
Unmeel B. Mehta‡
NASA Ames Research Center, Moffett Field, CA 94035

Abstract

A new parabolized Navier-Stokes (PNS) algorithm has been developed to efficiently compute magnetohydrodynamic (MHD) flows in the low magnetic Reynolds number regime. In this regime, the electrical conductivity is low and the induced magnetic field is negligible compared to the applied magnetic field. The MHD effects are modeled by introducing source terms into the PNS equation which can then be solved in a very efficient manner. To account for upstream (elliptic) effects, the flowfields are computed using multiple streamwise sweeps with an iterated PNS algorithm. Turbulence has been included by modifying the Baldwin-Lomax turbulence model to account for MHD effects. The new algorithm has been used to compute both laminar and turbulent, supersonic, MHD flows over flat plates and supersonic viscous flows in a rectangular MHD accelerator. The present results are in excellent agreement with previous complete Navier-Stokes calculations.

Introduction

Flowfields involving MHD effects have typically been computed [1–10] by solving the complete Navier-Stokes (N-S) equations for fluid flow in conjunction with Maxwell's equations of electromagnetodynamics. When chemistry and turbulence effects are also included, the computational effort required to solve the resulting coupled system of partial differential equations is extremely formidable. One possible remedy to this problem is to use the parabolized Navier-Stokes (PNS) equations in place of the N-S equations. The PNS equations can be used to compute three-dimensional, supersonic viscous flowfields in a very efficient manner [11]. This efficiency is achieved because the equations can be solved using a space-marching technique as opposed to the time-marching technique that is normally employed for the complete N-S equations.

Recently, the present authors have developed a PNS code to solve supersonic MHD flowfields in the high magnetic Reynolds number regime [12]. This code is based on NASA's upwind PNS (UPS) code which was originally developed by Lawrence et al. [13]. The UPS code solves the PNS equations using a fully conservative, finite-volume approach in a general nonorthogonal coordinate system. The UPS code has been extended to permit the computation of flowfields with strong upstream influences. In regions where strong upstream influences are present, the governing equations are solved using multiple sweeps. As a result of this approach, a complete flowfield can be computed more efficiently (in terms of computer time and storage) than with a standard N-S solver which marches the entire solution in time. Three iterative PNS algorithms (IPNS, TIPNS, and FBIPNS) have been developed. The iterated PNS (IPNS) algorithm [14] can be applied to flows with moderate upstream influences and small streamwise separated regions. The time iterated PNS (TIPNS) algorithm [15] can be used to compute flows with strong upstream influences including large streamwise separated regions. The forward-backward sweeping iterative PNS (FBIPNS) algorithm [16] was recently developed to reduce the number of sweeps required for convergence.

The majority of MHD codes that have been developed combine the electromagnetodynamic equations with the full Navier-Stokes equations resulting in a complex system of eight scalar equations.

*Graduate Research Assistant, Student Member AIAA
†Manager, Computational Fluid Dynamics Center, and Professor, Dept. of AEEM. Fellow AIAA
‡Division Scientist, Associate Fellow, AIAA

These codes can theoretically be used for any magnetic Reynolds number which is defined as $Re_m = \sigma_e \mu_e V_\infty L$ where σ_e is the electrical conductivity, μ_e is the magnetic permeability, V_∞ is the freestream velocity, and L is the reference length. However, it has been shown that as the magnetic Reynolds number is reduced, numerical difficulties are often encountered [4]. For many aerospace applications the electrical conductivity of the fluid is low and hence the magnetic Reynolds number is small. In these cases, it makes sense to use the low magnetic Reynolds number assumption and reduce the complexity of the governing equations. In this case, the MHD effects can be modeled with the introduction of source terms into the fluid flow equations. Several investigators [4, 8, 17–19] have developed N-S codes for the low magnetic Reynolds number regime where the induced magnetic field is negligible compared to the applied magnetic field.

In the present study, a new PNS code (based on the UPS code) has been developed to compute MHD flows in the low magnetic Reynolds number regime. The MHD effects are modeled by introducing the appropriate source terms into the PNS equations. Upstream elliptic effects can be accounted for by using multiple streamwise sweeps with either the IPNS, TIPNS, or FBIPNS algorithms. Turbulence has been included by modifying the Baldwin-Lomax turbulence model [20] to account for MHD effects using the approach of Lykoudis [21]. The new code has been tested by computing both laminar and turbulent, supersonic MHD flows over a flat plate. Comparisons have been made with the previous complete N-S computations of Dietiker and Hoffmann [18]. In addition, the new code has been used to compute the supersonic viscous flow inside a rectangular channel designed for MHD experiments [22].

Governing Equations

The governing equations for a viscous MHD flow with a small magnetic Reynolds number are given by [18]:
Continuity equation

$$\frac{\partial \rho}{\partial t} + \nabla \cdot (\rho \mathbf{V}) = 0 \tag{1}$$

Momentum equation

$$\frac{\partial (\rho \mathbf{V})}{\partial t} + \nabla \cdot \left[\rho \mathbf{V}\mathbf{V} + p\bar{\bar{\mathbf{I}}}\right] = \nabla \cdot \bar{\bar{\tau}} + \mathbf{J} \times \mathbf{B} \tag{2}$$

Energy equation

$$\frac{\partial (\rho e_t)}{\partial t} + \nabla \cdot [(\rho e_t + p)\,\mathbf{V}]$$
$$= \nabla \cdot (\mathbf{V} \cdot \bar{\bar{\tau}}) - \nabla \cdot \mathbf{U} + \mathbf{E} \cdot \mathbf{J} \tag{3}$$

Ohm's law

$$\mathbf{J} = \sigma_e \left(\mathbf{E} + \mathbf{V} \times \mathbf{B}\right) \tag{4}$$

where $\mathbf{V}$ is the velocity vector, $\mathbf{B}$ is the magnetic field vector, $\mathbf{E}$ is the electric field vector, and $\mathbf{J}$ is the conduction current density. The flow is assumed to be either in chemical equilibrium or in a frozen state. The curve fits of Srinivasan et al. [23, 24] are used for the thermodynamic and transport properties of equilibrium air.

The governing equations are nondimensionalized using the following reference variables.

$$x^*, y^*, z^* = \frac{x, y, z}{L}\,, \quad u^*, v^*, w^* = \frac{u, v, w}{U_\infty}\,, \quad t^* = \frac{U_\infty t}{L}$$

$$\rho^* = \frac{\rho}{\rho_\infty}\,, \quad T^* = \frac{T}{T_\infty}\,, \quad p^* = \frac{p}{\rho_\infty U_\infty^2}$$

$$e_t^* = \frac{e_t}{U_\infty^2}\,, \quad \bar{\bar{\tau}}^* = \frac{\bar{\bar{\tau}} L}{\mu_\infty U_\infty}\,, \quad \mu^* = \frac{\mu}{\mu_\infty} \tag{5}$$

$$B_x^*, B_y^*, B_z^* = \frac{B_x, B_y, B_z}{U_\infty \sqrt{\mu_e \rho_\infty}}\,, \quad E_x^*, E_y^*, E_z^* = \frac{E_x, E_y, E_z}{U_\infty^2 \sqrt{\mu_e \rho_\infty}}$$

$$\mu_e^* = \frac{\mu_e}{\mu_{e\infty}} = 1\,, \quad \sigma_e^* = \frac{\sigma_e}{\sigma_{e\infty}}$$

where the superscript $*$ refers to the nondimensional quantities. In subsequent sections, the asterisks are dropped.

If the flow variables are assumed to vary in only two dimensions (x, y) while the velocity, magnetic, and electric fields have components in three dimensions (x, y, z), the governing equations can be written in the following flux vector form:

$$\frac{\partial \mathbf{U}}{\partial t} + \frac{\partial \mathbf{E}_i}{\partial x} + \frac{\partial \mathbf{F}_i}{\partial y} = \frac{\partial \mathbf{E}_v}{\partial x} + \frac{\partial \mathbf{F}_v}{\partial y} + \mathbf{S}_{\text{MHD}} \tag{6}$$

where $\mathbf{U}$ is the vector of dependent variables and $\mathbf{E}_i$ and $\mathbf{F}_i$ are the inviscid flux vectors, and $\mathbf{E}_v$ and $\mathbf{F}_v$ are the viscous flux vectors. The source term $\mathbf{S}_{\text{MHD}}$ contains all of the MHD effects. The flux vectors are given by

$$\mathbf{U} = \left[\ \rho,\ \ \rho u,\ \ \rho v,\ \ \rho w,\ \ \rho e_t\ \right]^T \tag{7}$$

$$\mathbf{E}_i = \begin{bmatrix} \rho u \\ \rho u^2 + p \\ \rho uv \\ \rho uw \\ (\rho e_t + p)u \end{bmatrix}\,, \quad \mathbf{F}_i = \begin{bmatrix} \rho v \\ \rho uv \\ \rho v^2 + p \\ \rho vw \\ (\rho e_t + p)v \end{bmatrix} \tag{8}$$

$$\mathbf{E}_v = \begin{bmatrix} 0 \\ \tau_{xx} \\ \tau_{xy} \\ \tau_{xz} \\ u\tau_{xx} + v\tau_{xy} + w\tau_{xz} - q_x \end{bmatrix} \quad (9)$$

$$\mathbf{F}_v = \begin{bmatrix} 0 \\ \tau_{yx} \\ \tau_{yy} \\ \tau_{yz} \\ u\tau_{yx} + v\tau_{yy} + w\tau_{yz} - q_y \end{bmatrix} \quad (10)$$

$$\mathbf{S}_{\text{MHD}} = Re_m \begin{bmatrix} 0 \\ \hline B_z(E_y + wB_x - uB_z) \\ -B_y(E_z + uB_y - vB_x) \\ \hline B_x(E_z + uB_y - vB_x) \\ -B_z(E_x + vB_z - wB_y) \\ \hline B_y(E_x + vB_z - wB_y) \\ -B_x(E_y + wB_x - uB_z) \\ \hline E_x(E_x + vB_z - wB_y) \\ +E_y(E_y + wB_x - uB_z) \\ +E_z(E_z + uB_y - vB_x) \end{bmatrix} \quad (11)$$

where

$$\rho e_t = \frac{1}{2}\rho\left(u^2 + v^2 + w^2\right) + \frac{p}{\tilde{\gamma} - 1} \quad (12)$$

and $\tilde{\gamma}$ can be determined from the curve fits of Srinivasan et al. [23] for an equilibrium air flow or is equal to a constant (γ) for a frozen or perfect gas flow. The nondimensional shear stresses and heat fluxes are defined in the usual manner [11].

The governing equations are transformed into computational space and written in a generalized coordinate system (ξ, η) as

$$\frac{1}{J}\mathbf{U}_t + \mathbf{E}_\xi + \mathbf{F}_\eta = \frac{\mathbf{S}_{\text{MHD}}}{J} \quad (13)$$

where

$$\begin{aligned} \mathbf{E} &= \left(\frac{\xi_x}{J}\right)(\mathbf{E}_i - \mathbf{E}_v) + \left(\frac{\xi_y}{J}\right)(\mathbf{F}_i - \mathbf{F}_v) \\ \mathbf{F} &= \left(\frac{\eta_x}{J}\right)(\mathbf{E}_i - \mathbf{E}_v) + \left(\frac{\eta_y}{J}\right)(\mathbf{F}_i - \mathbf{F}_v) \end{aligned} \quad (14)$$

and J is the Jacobian of the transformation.

The governing equations are parabolized by dropping the time derivative term and the streamwise direction (ξ) viscous flow terms in the flux vectors. Equation (13) can then be rewritten as

$$\mathbf{E}_\xi + \mathbf{F}_\eta = \frac{\mathbf{S}_{\text{MHD}}}{J} \quad (15)$$

where

$$\begin{aligned} \mathbf{E} &= \left(\frac{\xi_x}{J}\right)\mathbf{E}_i + \left(\frac{\xi_y}{J}\right)\mathbf{F}_i \\ \mathbf{F} &= \left(\frac{\eta_x}{J}\right)(\mathbf{E}_i - \mathbf{E}'_v) + \left(\frac{\eta_y}{J}\right)(\mathbf{F}_i - \mathbf{F}'_v) \end{aligned} \quad (16)$$

The prime in the preceding equation indicates that the streamwise viscous flow terms have been dropped.

For turbulent flows, the two-layer Baldwin-Lomax turbulence model [20] has been modified to account for MHD effects. Only the expression for turbulent viscosity in the inner layer is changed. This modification for MHD flows is due to Lykoudis [9, 21].

Numerical Method

The governing PNS equations with MHD source terms have been incorporated into NASA's upwind PNS (UPS) code [13]. These equations can be solved very efficiently using a single sweep of the flowfield for many applications. For cases where upstream (elliptic) effects are important, the flowfield can be computed using multiple streamwise sweeps with either the IPNS [14], TIPNS [15], or FBIPNS [16] algorithms. This iterative process is continued until the solution is converged.

For the iterative PNS (IPNS) method, the $\mathbf{E}$ vector is split using the Vigneron parameter (ω) [25]. This parameter does not need to be changed for the present low magnetic Reynolds number formulation. In the previous high magnetic Reynolds number code [12] it was necessary to modify the Vigneron parameter to account for MHD effects. After splitting, the $\mathbf{E}$ vector can be written as:

$$\mathbf{E} = \mathbf{E}^* + \mathbf{E}^p \quad (17)$$

where

$$\begin{aligned} \mathbf{E}^* &= \frac{\xi_x}{J}\begin{bmatrix} \rho u \\ \rho u^2 + \omega p \\ \rho uv \\ \rho uw \\ (\rho e_t + p)\, u \end{bmatrix} + \frac{\xi_y}{J}\begin{bmatrix} \rho v \\ \rho uv \\ \rho v^2 + \omega p \\ \rho vw \\ (\rho e_t + p)\, v \end{bmatrix} \\ \mathbf{E}^p &= \frac{\xi_x}{J}\begin{bmatrix} 0 \\ (1-\omega)p \\ 0 \\ 0 \\ 0 \end{bmatrix} + \frac{\xi_y}{J}\begin{bmatrix} 0 \\ 0 \\ (1-\omega)p \\ 0 \\ 0 \end{bmatrix} \end{aligned} \quad (18)$$

The streamwise derivative of $\mathbf{E}$ is then differenced using a forward difference for the "elliptic" portion ($\mathbf{E}^p$):

$$\left(\frac{\partial \mathbf{E}}{\partial \xi}\right)_{i+1} = \frac{1}{\Delta\xi}\left[\left(\mathbf{E}^*_{i+1} - \mathbf{E}^*_i\right) + \left(\mathbf{E}^p_{i+2} - \mathbf{E}^p_{i+1}\right)\right] \quad (19)$$

where the subscript $(i+1)$ denotes the spatial index (in the ξ direction) where the solution is currently being computed. The vectors $\mathbf{E}^*_{i+1}$ and $\mathbf{E}^p_{i+1}$ are then linearized in the following manner:

$$\begin{aligned} \mathbf{E}^*_{i+1} &= \mathbf{E}^*_i + \left(\frac{\partial \mathbf{E}^*}{\partial \mathbf{U}}\right)_i (\mathbf{U}_{i+1} - \mathbf{U}_i) \\ \mathbf{E}^p_{i+1} &= \mathbf{E}^p_i + \left(\frac{\partial \mathbf{E}^p}{\partial \mathbf{U}}\right)_i (\mathbf{U}_{i+1} - \mathbf{U}_i) \end{aligned} \quad (20)$$

The Jacobians can be represented by

$$\begin{aligned} A^* &= \frac{\partial \mathbf{E}^*}{\partial \mathbf{U}} \\ A^p &= \frac{\partial \mathbf{E}^p}{\partial \mathbf{U}} \end{aligned} \quad (21)$$

After substituting the above linearizations into Eq. (19), the expression for the streamwise gradient of $\mathbf{E}$ becomes

$$\left(\frac{\partial \mathbf{E}}{\partial \xi}\right)_{i+1} = \frac{1}{\Delta\xi}\Big[(A^*_i - A^p_i)(\mathbf{U}_{i+1} - \mathbf{U}_i) + (\mathbf{E}^p_{i+2} - \mathbf{E}^p_i)\Big] \quad (22)$$

The final discretized form of the fluid flow equations with MHD source terms is obtained by substituting Eq. (22) into Eq. (15) along with the linearized expression for the flux in the cross flow plane. The final expression becomes:

$$\left[\frac{1}{\Delta\xi}(A^*_i - A^p_i) + \frac{\partial}{\partial\eta}\left(\frac{\partial \mathbf{F}}{\partial \mathbf{U}}\right)_i\right]^{k+1} (\mathbf{U}_{i+1} - \mathbf{U}_i)^{k+1} = \mathbf{RHS} \quad (23)$$

where

$$\mathbf{RHS} = -\frac{1}{\Delta\xi}\left[(\mathbf{E}^p_{i+2})^k - (\mathbf{E}^p_i)^{k+1}\right] - \left(\frac{\partial \mathbf{F}}{\partial \eta}\right)^{k+1}_i + \left(\frac{\mathbf{S}_{\mathrm{MHD}}}{J}\right)^k_{i+1}$$

and the superscript k+1 denotes the current iteration (i.e. sweep) level.

Numerical Results

In order to investigate the utility and accuracy of the present PNS approach of solving MHD flowfields at low magnetic Reynolds numbers, a few basic test cases were computed. The supersonic viscous flow in these cases is altered by the presence of the magnetic and electric fields which are applied to the flow.

Test Case 1: Supersonic laminar and turbulent flows over a flat plate with applied magnetic field

In this test case, the supersonic, laminar and turbulent flow over a flat plate with an applied magnetic field is computed. This case corresponds to the flat plate case computed previously by Dietiker and Hoffmann [18] using the full N-S equations. A strong magnetic field is applied normal to the flow as shown in Fig. 1. The dimensional flow parameters for this test case are:

$$\begin{aligned} M_\infty &= 2.0 \\ p_\infty &= 1.076 \times 10^5 \ \mathrm{N/m^2} \\ T_\infty &= 300 \ \mathrm{K} \\ Re_\infty &= 3.75 \times 10^6 \\ \gamma &= 1.4 \\ L &= 0.08 \ \mathrm{m} \\ \sigma_e &= 800 \ \mathrm{mho/m} \end{aligned}$$

The plate is assumed to be an adiabatic wall and a perfect gas flow is assumed. The magnetic Reynolds number (based on the length of the plate) is 0.056 and can be considered negligible when compared to one. The normal magnetic field component (B_y) ranges in value from 0.0 to 1.2 T. The magnitude of the magnetic field can be represented by the parameter m which is defined [18] by

$$m = \frac{\sigma_e B_y^2}{\rho_\infty U_\infty} \quad (24)$$

and has units of $(1/m)$. For $B_y = 1.2$ T, m is equal to 1.33.

A highly stretched grid consisting of 50 points in the normal direction was used to compute this case. The first point off the wall was located at 2×10^{-7} m. Initially, the flow was assumed laminar and several values of B_y ranging from 0.0 (no magnetic field) to 1.2 T were used. The velocity and temperature profiles at $x = 0.06$ m are shown in Figs. 2 and 3 for $B_y = 0.0$ T, 1.0 T, and 1.2 T. The velocity profiles are compared to the N-S results of Dietiker and Hoffmann in Fig. 2 and show excellent agreement. The magnetic field generates a Lorentz force which acts in a direction opposite to the flow. Thus, the flow is decelerated as the magnetic field is increased as seen in Fig. 2. For $B_y = 1.2$ T the flow is slightly separated. The temperature profiles cannot be compared at this time since no temperature data is given in Ref. [18].

The turbulent flow over the flat plate was then computed using the modified Baldwin-Lomax turbulence model that accounts for MHD effects. The flow

was assumed laminar prior to the point ($x = 0.04$ m) where transition from laminar to turbulent flow was triggered. Again, several values of B_y ranging from 0.0 to 1.2 T were used in the computations. The turbulent velocity and temperature profiles at $x = 0.06$ m are shown in Figs. 4 and 5 for $B_y = 0.0$, 1.0 T, and 1.2 T. The turbulent velocity profiles in Fig. 4 are in good agreement with the results of Ref. [18]. The variation of skin friction coefficient is shown in Fig. 6. The present laminar/turbulent skin friction variations are compared with the results of Ref. [18] and show good agreement. The difference in results near the transition point may be due to the coarse grid and smoothing used in Ref. [18].

All of the present laminar computations were performed using a single sweep of the flowfield except for the separated flow case ($B_y = 1.2$ T). For this case as well as for all the turbulent cases, multiple sweeps were used to account for upstream effects.

Test Case 2: Supersonic viscous flow in a rectangular MHD accelerator

In this test case, the supersonic flow in an experimental MHD channel is simulated. This facility is currently being built at NASA Ames Research Center by D. W. Bogdanoff, C. Park, and U. B. Mehta [22] to study critical technologies related to MHD bypass scramjet engines. The channel is about a half meter long and contains a nozzle section, a center section, and an accelerator section. The channel has a uniform width of 2.03 cm. Magnetic and electric fields can be imposed upon the flow in the accelerator section. A schematic of the MHD accelerator section is shown in Fig. 7.

This test case was previously computed by R. W. MacCormack [10] using the full N-S equations coupled with the electromagnetodynamic equations. The electrical conductivity in his calculations was set at 1.0×10^5 mho/m resulting in a very large magnetic Reynolds number. In the present study, the calculations are performed in the low magnetic Reynolds number regime using a realistic value of electrical conductivity. The flow is computed in two dimensions, but later will be extended to three dimensions. Because of flow symmetry, only half of the channel is computed in the 2-D calculations.

The flow in the nozzle section and the center section was computed using a combination of the OVERFLOW code [26] and the present PNS code (without MHD effects). The initial conditions for the nozzle (flow at rest) were:

$$p_0 = 8.0 \times 10^5 \text{ N/m}^2$$

$$T_0 = 7500 \text{ K}$$

The laminar flow was assumed to be in chemical equilibrium. The computed flowfield at the end of the center section was then used as the starting solution for the flow calculation of the accelerator section. The MHD parameters used in the accelerator section were:

$$\begin{aligned} \sigma_e &= 50 \text{ mho/m} \\ B_y &= 1.5 \text{ T} \\ E_z &= -K u_c B_y \\ Re_m &= 0.05 \end{aligned}$$

where the load factor (K) ranged in values from 0.0 to 1.4, and the centerline velocity (u_c) at the beginning of the accelerator section had a value of 3162 m/s.

The velocity profiles at the end of the accelerator section are shown in Fig. 8 for different load factors. The velocity profile with no electric or magnetic fields is denoted by $K = 0$. The increase in the centerline velocity with distance (x) for various load factors is shown in Fig. 9. The centerline velocity increases by about 30% with a load factor of 1.4. It should be noted that the flow decelerates because of friction when no electric or magnetic fields are applied.

Concluding Remarks

In this study, a new parabolized Navier-Stokes algorithm has been developed to efficiently compute MHD flows in the low magnetic Reynolds number regime. The new algorithm has been used to compute both laminar and turbulent, supersonic, MHD flows over flat plates and in a rectangular accelerator section. Although only limited results have been obtained thus far, it can be seen that the present approach is quite promising. Computations of other test cases are currently underway in order to validate the current method.

Acknowledgments

This work was supported by NASA Ames Research Center under Grants NCC2-5379 and NCC2-5517 and by Iowa State University. The Technical Monitor for the NASA grant is Dr. Unmeel B. Mehta.

References

[1] Gaitonde, D. V., "Development of a Solver for 3-D Non-Ideal Magnetogasdynamics," AIAA Paper 99-3610, June 1999.

[2] Damevin, H. M., Dietiker, J.-F., and Hoffmann, K. A., "Hypersonic Flow Computations with Magnetic Field," AIAA Paper 2000-0451, Jan. 2000.

[3] Hoffmann, K. A., Damevin, H. M., and Dietiker, J.-F., "Numerical Simulation of Hypersonic Magnetohydrodynamic Flows," AIAA Paper 2000-2259, June 2000.

[4] Gaitonde, D. V. and Poggie, J., "Simulation of MHD Flow Control Techniques," AIAA Paper 2000-2326, June 2000.

[5] MacCormack, R. W., "Numerical Computation in Magnetofluid Dynamics," *Computational Fluid Dynamics for the 21st Century*, Kyoto, Japan, July 2000.

[6] Deb, P. and Agarwal, R., "Numerical Study of MHD-Bypass Scramjet Inlets with Finite-Rate Chemistry," AIAA Paper 2001-0794, Jan. 2001.

[7] MacCormack, R. W., "A Computational Method for Magneto-Fluid Dynamics," AIAA Paper 2001-2735, June 2001.

[8] Gaitonde, D. V. and Poggie, J., "An Implicit Technique for 3-D Turbulent MGD with the Generalized Ohm's Law," AIAA Paper 2001-2736, June 2001.

[9] Dietiker, J.-F. and Hoffmann, K. A., "Numerical Simulation of Turbulent Magnetohydrodynamic Flows," AIAA Paper 2001-2737, June 2001.

[10] MacCormack, R. W., "Three Dimensional Magneto-Fluid Dynamics Algorithm Development," AIAA Paper 2002-0197, Jan. 2002.

[11] Tannehill, J. C., Anderson, D. A., and Pletcher, R. H., *Computational Fluid Mechanics and Heat Transfer*, Taylor and Francis, Washington, D.C., 1997.

[12] Kato, H., Tannehill, J. C., Ramesh, M. D., and Mehta, U. B., "Computation of Magnetohydrodynamic Flows Using an Iterative PNS Algorithm," AIAA Paper 2002-0202, Jan. 2002.

[13] Lawrence, S. L., Tannehill, J. C., and Chaussee, D. S., "Upwind Algorithm for the Parabolized Navier-Stokes Equations," *AIAA Journal*, Vol. 27, No. 9, Sept. 1989, pp. 1975–1983.

[14] Miller, J. H., Tannehill, J. C., and Lawrence, S. L., "PNS Algorithm for Solving Supersonic Flows with Upstream Influences," AIAA Paper 98-0226, Jan. 1998.

[15] Tannehill, J. C., Miller, J. H., and Lawrence, S. L., "Development of an Iterative PNS Code for Separated Flows," AIAA Paper 99-3361, June 1999.

[16] Kato, H. and Tannehill, J. C., "Development of a Forward-Backward Sweeping Parabolized Navier-Stokes Algorithm," AIAA Paper 2002-0735, Jan. 2002.

[17] Munipalli, R., Anderson, D. A., and Kim, H., "Two-Temperature Computations of Ionizing Air with MHD Effects," AIAA Paper 2000-0450, Jan. 2000.

[18] Dietiker, J.-F. and Hoffmann, K. A., "Boundary Layer Control in Magnetohydrodynamic Flows," AIAA Paper 2002-0130, Jan. 2002.

[19] Cheng, F., Zhong, X., Gogineni, S., and Kimmel, R. L., "Effect of Applied Magnetic Field on the Instability of Mach 4.5 Boundary Layer over a Flat Plate," AIAA Paper 2002-0351, Jan. 2002.

[20] Baldwin, B. S. and Lomax, H., "Thin Layer Approximation and Algebraic Model for Separated Turbulent Flows," AIAA-Paper 78-257, Jan. 1978.

[21] Lykoudis, P. S., "Magneto Fluid Mechanics Channel Flow, II Theory," *The Physics of Fluids*, Vol. 10, No. 5, May 1967, pp. 1002–1007.

[22] Bogdanoff, D. W., Park, C., and Mehta, U. B., "Experimental Demonstration of Magneto-Hydrodynamic (MHD) Acceleration - Facility and Conductivity Measurements," NASA TM-2001-210922, July 2001.

[23] Srinivasan, S., Tannehill, J. C., and Weilmuenster, K. J., "Simplified Curve Fits for the Thermodynamic Properties of Equilibrium Air," NASA RP 1181, Aug. 1987.

[24] Srinivasan, S., Tannehill, J. C., and Weilmuenster, K. J., "Simplified Curve Fits for the Transport Properties of Equilibrium Air," NASA CR 178411, 1987.

[25] Vigneron, Y. C., Rakich, J. V., and Tannehill, J. C., "Calculation of Supersonic Flow over Delta Wings with Sharp Subsonic Leading Edges," AIAA Paper 78-1137, July 1978.

[26] Buning, P. G., Jespersen, D. C., and Pulliam, T. H., *OVERFLOW Manual, Version 1.7v*, NASA Ames Research Center, Moffett Field, California, June 1997.

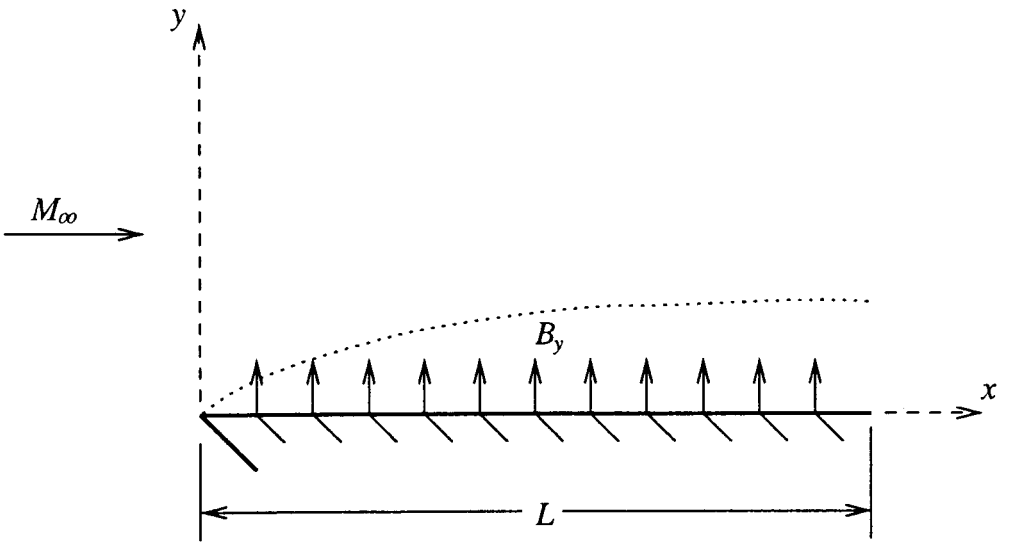

Figure 1: Test Case 1

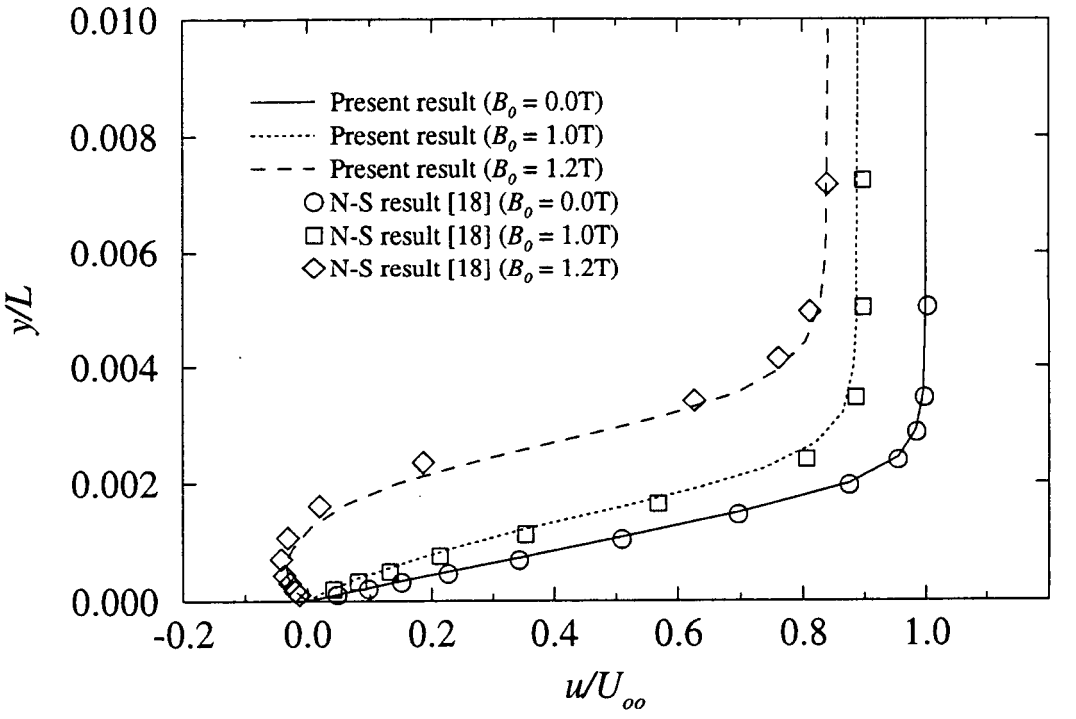

Figure 2: Laminar velocity profiles

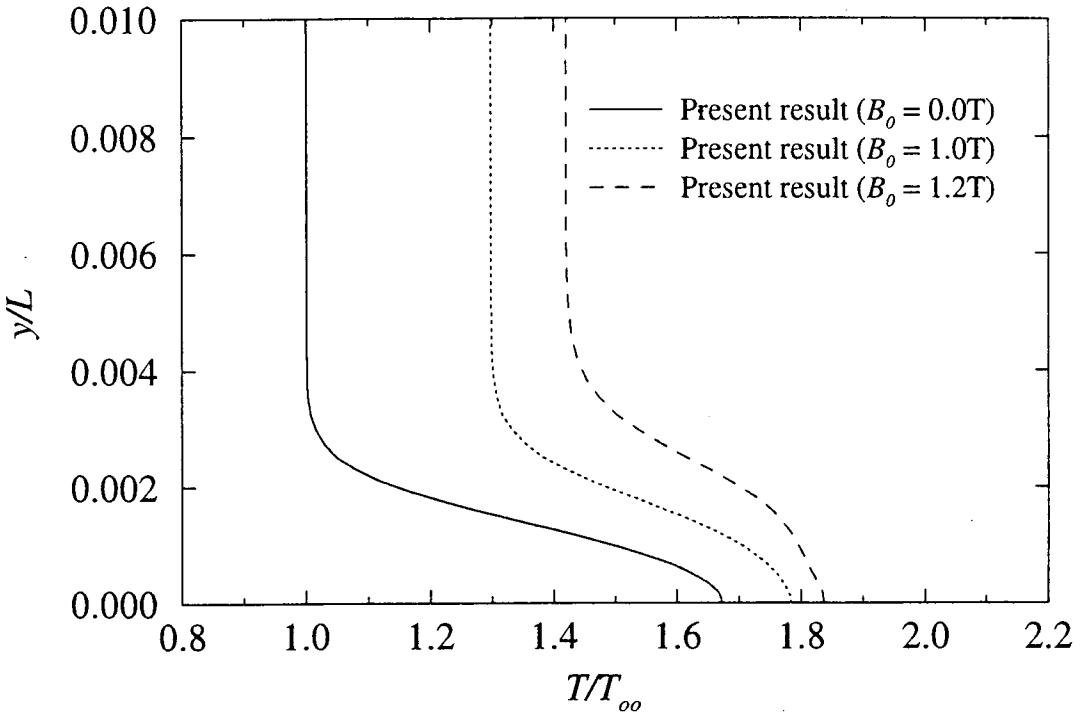

Figure 3: Laminar temperature profiles

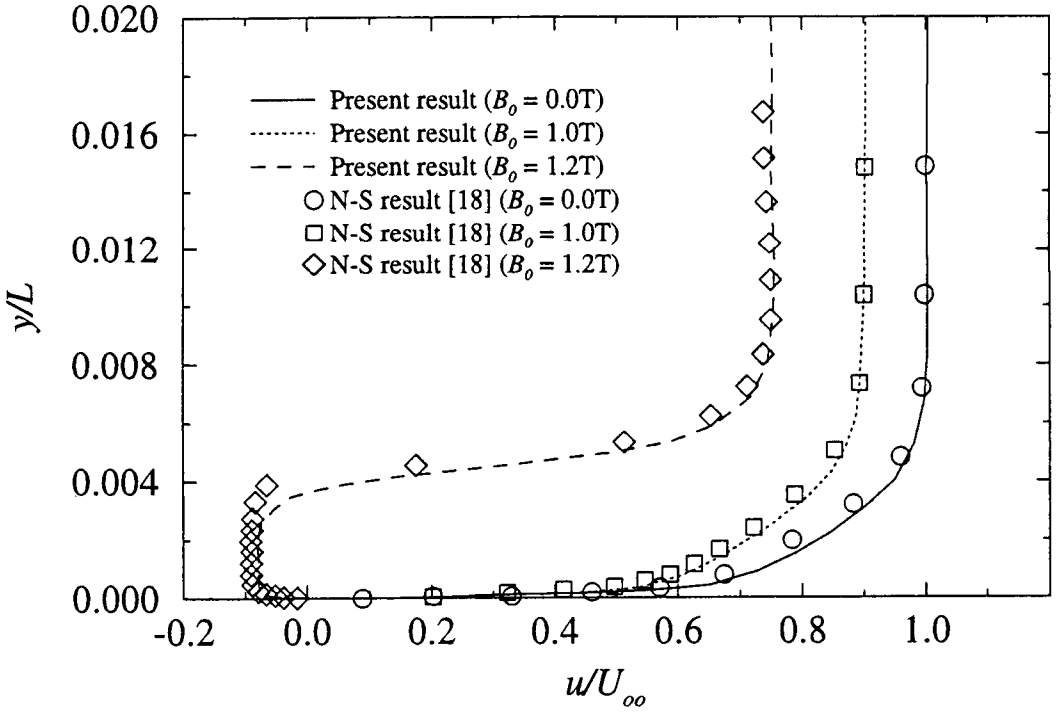

Figure 4: Turbulent velocity profiles

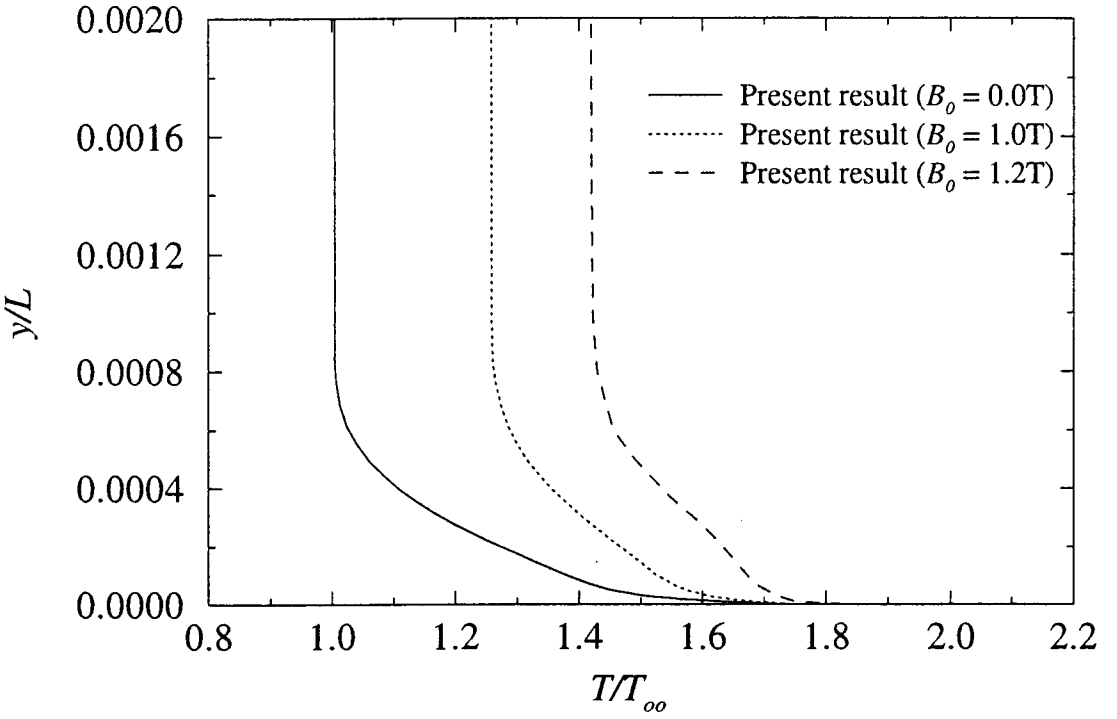

Figure 5: Turbulent temperature profiles

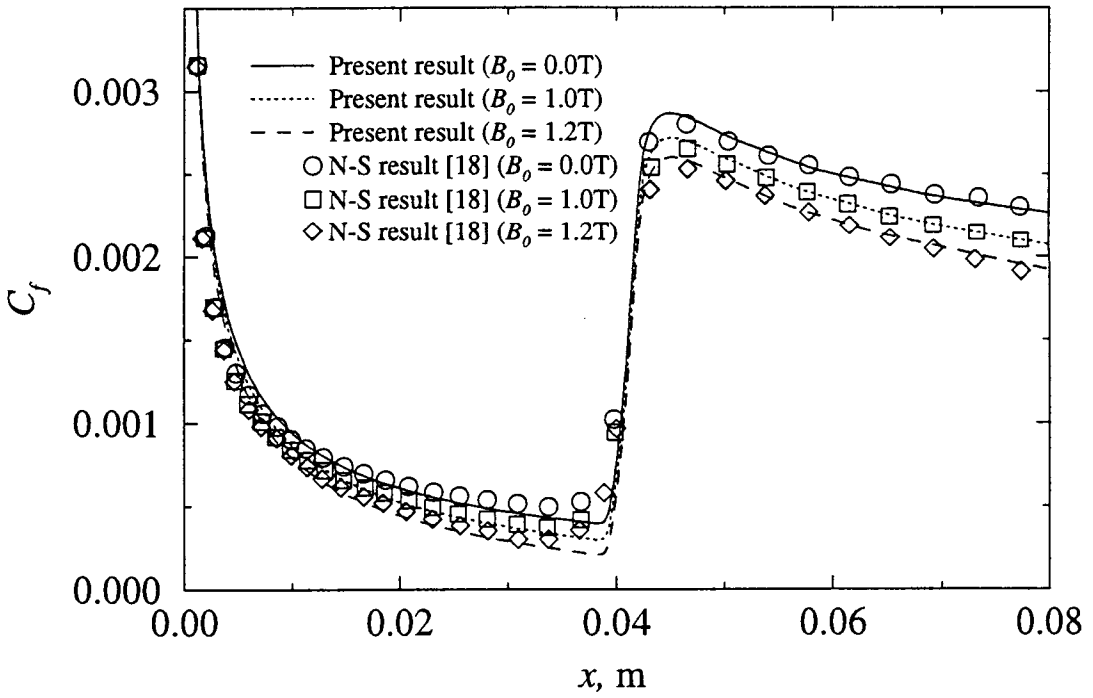

Figure 6: Laminar/turbulent skin friction coefficient

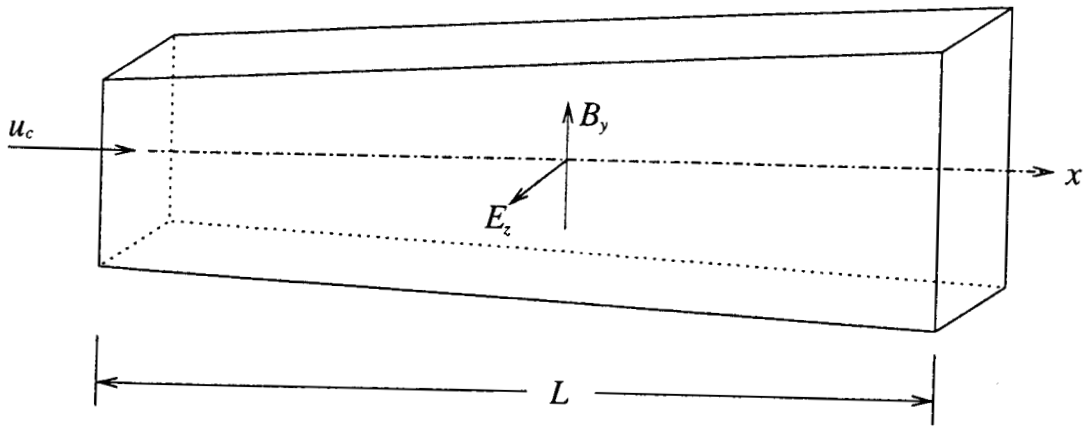

Figure 7: Schematic of MHD accelerator section

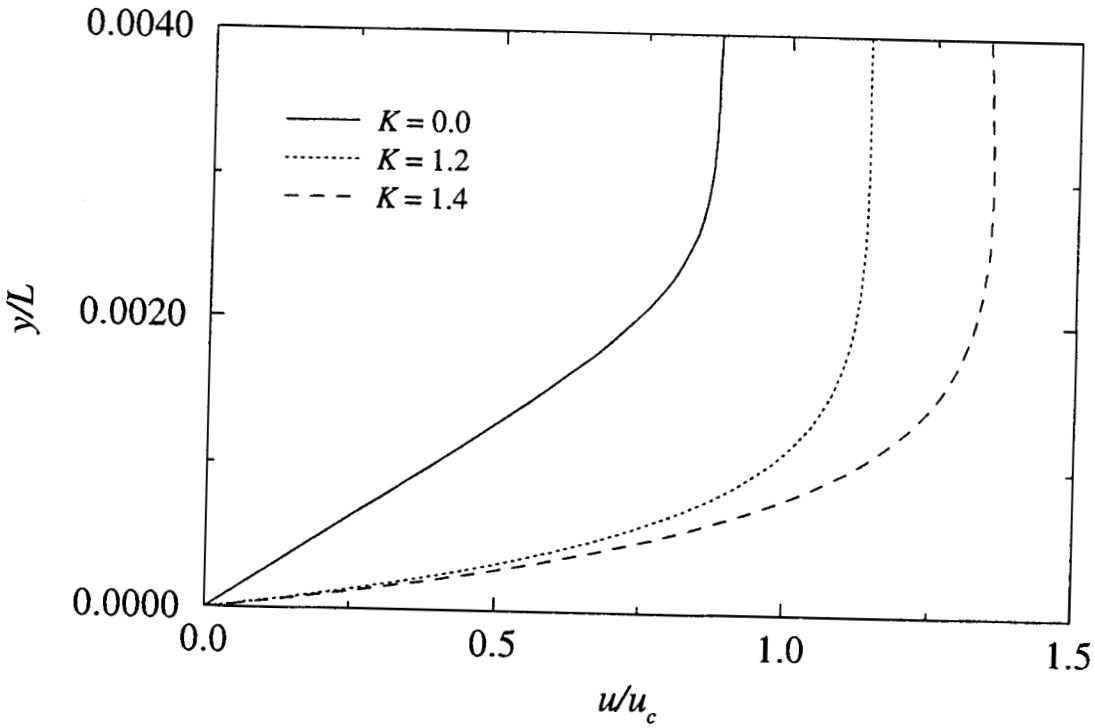

Figure 8: Velocity profiles at end of accelerator

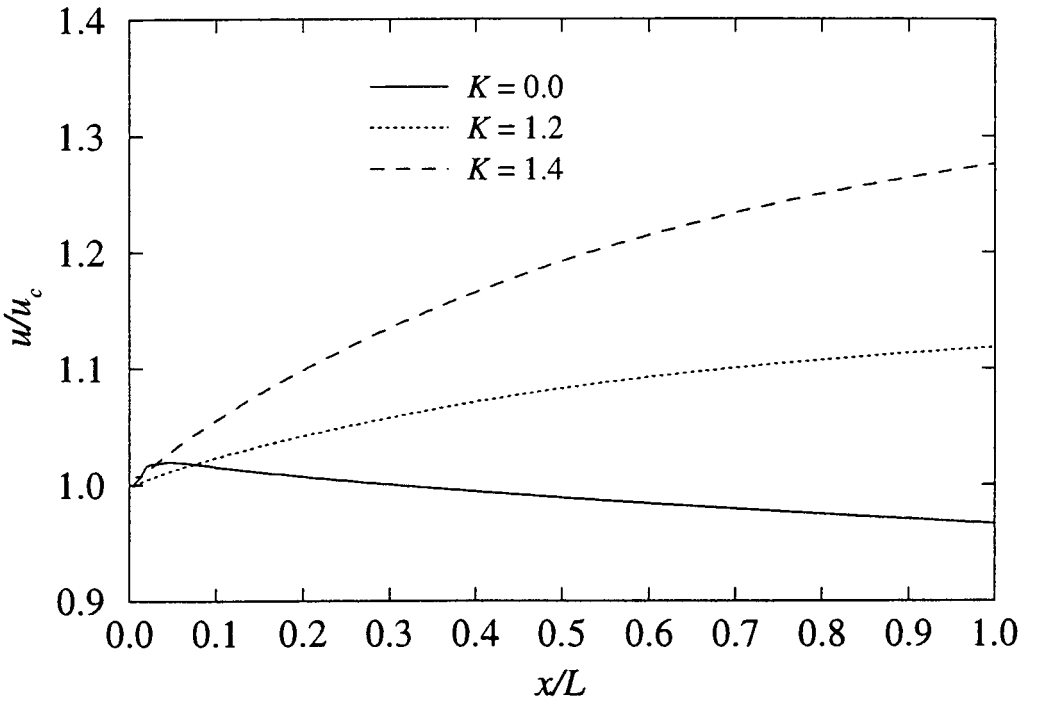

Figure 9: Centerline velocity for various load factors